Hypoosmotic- and pressure-induced membrane stretch activate TRPC5 channels

Ana Gomis*, Sergio Soriano, Carlos Belmonte and Félix Viana,

Instituto de Neurociencias de Alicante, Consejo Superior de Investigaciones Científicas-Universidad Miguel Hernández, Alicante, Spain

*To whom correspondence should be addressed at: Instituto de Neurociencias de Alicante, Consejo Superior de Investigaciones Científicas-Universidad Miguel Hernández. Carretera de Valencia, N-332, Km 113. 03550 Sant Joan d'Alacant, Alicante, Spain. E-mail: agomis@umh.es.

Abbreviated title: Osmo-mechanical activation of TRPC5

Number of figures: 8

Keywords: TRP channel, osmosensitivity, PIP_2, sensory transduction, GsMTx-4 peptide, mechanotransduction

INTRODUCTION

Transient receptor potential (TRP) cation channels are emerging as important molecular elements of sensory transduction events (Clapham, 2003; Voets *et al.*, 2005). TRP channels play key roles in nociception, photo-, chemo-, thermo- and mechano-osmotic transduction (Dhaka *et al.*, 2006; Venkatachalam & Montell, 2007). The detection of mechanical stimuli is essential for basic physiological functions such as touch, hearing, myogenic vascular tone, muscle stretch, and volume regulation by the kidney (Hamill & Martinac, 2001; Kung, 2005). Several TRP channels are sensitive to various forms of mechanical stress, including the increase in membrane surface tension produced by osmotic swelling (Pedersen & Nilius, 2007; Christensen & Corey, 2007; Raoux M *et al.*, 2007). TRPV4 was the first TRP channel to be described as activated by osmotic cell swelling (Strotmann *et al.*, 2000; Liedtke *et al.*, 2000). This activation is not due to direct stretch but is mediated by 5',6'-epoxyeicosatrienoic acid (5',6'-EET), a metabolite of arachidonic acid (Watanabe *et al.*, 2003; Vriens *et al.*, 2004). TRPV2 is also activated by osmotic cell swelling (Muraki *et al.*, 2003; Beech *et al.*, 2004) and responds to stretch in vascular smooth muscle cells although its mechanism of activation remains unclear. TRPM4 (Dietrich *et al.*, 2006; Earley *et al.*, 2004; Kraft & Harteneck, 2005; Inoue *et al.*, 2006), and a long splice variant of TRPM3 (Grimm et al., 2003) are also activated by hypotonic cell swelling. Among the TRPC family, TRPC1 and TRPC6 are activated by mechanically or osmotically induced membrane stretch (Maroto *et al.*, 2005; Spassova *et al.*, 2006), which led these authors to hypothesize a role of TRPC6 in the regulation of myogenic vascular tone. However, more recent reports have challenged the mechanical gating of TRPC6 and TRPC1 channels (Dietrich *et al.*, 2007; Gottlieb *et al.*, 2008; Sharif-Naeini *et al.*, 2008).

TRPC5 and its close homolog TRPC4 form group 4 of mammalian TRPC channels (Plant & Schaefer, 2003). TRPC5 is highly expressed in the central nervous system (Fowler *et al.*, 2007) and at lower levels in many other tissues such as gonads, lung, heart, adrenal gland, endothelium, kidney and vascular and gastric smooth muscle (Philipp *et al.*, 1998; Okada *et al.*, 1998; Riccio *et al.*, 2002; Beech *et al.*, 2004). TRPC5 channels can be turned on by activating receptors that couple to PLC (Schaefer *et al.*, 2000; Putney, Jr., 2004). This activation is also dependent on Ca^{2+} (Okada *et al.*, 1998; Schaefer *et al.*, 2000). At present, there is very limited information on the physiological role of TRPC5 channels. In the brain, TRPC5 activity regulates neurite extension in the hippocampus by a mechanism involving recruitment of channels to the plasma membrane (Greka *et al.*, 2003). The activity of TRPC5 is also increased by extracellular acidity (Semtner *et al.*, 2007) although further studies are

necessary to establish the role of changes in pH in the regulation of TRPC5 activity in native tissues. More recently, it was found that extracellular reduced thioredoxin (rTRX) activates TRPC5 channels (Xu *et al.*, 2008). Elevated rTRX occurs in human joints affected by rheumatoid arthritis and its activity is correlated with disease severity (Maurice *et al.*, 1999; Lemarechal *et al.*, 2007). It has also been proposed that TRPC5 acts as a direct sensor of lysophospholipids (Flemming *et al.*, 2006), suggesting that this channel exhibits sensitivity to the structure of the lipid bilayer. TRPC5 is also present in baroreceptors (Glazebrook *et al.*, 2005), the peripheral nerve endings involved in sensing arterial pressure, thus making the channel a potential candidate protein for osmo-mechanical transduction.

In this work, we address the role of TRPC5 as a potential osmo-mechanical transducer channel. Our data demonstrate activation of TRPC5 by hypoosmotic and pressure induced membrane stretch. Moreover, hypoosmotic induced membrane stretch is blocked by GsMTx-4, an inhibitor of stretch and mechanical activated ion channels (Suchyna *et al.*, 2000; Park *et al.*, 2008). Activation of TRPC5 by membrane stretch is independent of PLC signalling although it requires permissive levels of PIP_2 in the plasma membrane. Our results reveal a novel activation pathway for TRPC5 channels. Moreover, prominent expression of this channel in trigeminal ganglion sensory neurones suggests a possible involvement of TRPC5 in mammalian osmo-mechanosensory transduction.

MATERIAL AND METHODS

Bathing solutions and reagents

We employed external solutions of different osmolarities, measured with a cryoscopic osmometer (Gonotec GmgH, Berlin, Germany). The isotonic bathing solution used for fluorimetric calcium measurements contained (in mM): 90 NaCl, 5 KCl, 1.3 $MgCl_2$, 2.4 $CaCl_2$, 10 HEPES, 10 D-glucose, with pH adjusted to 7.4 with NaOH. 100 mM mannitol was added to maintain osmolarity constant at 300 mOsm/Kg. The hypoosmotic solutions (260 and 210 mOsm/Kg) were prepared by reducing the final concentration of mannitol without changing the ionic composition. For the 170 mOsm/Kg solution [Na^+] was reduced to 70 mM compared to standard buffer. For Ca^{2+}- free solutions, calcium was omitted and replaced with 5 mM EGTA. Experiments were performed at RT (22-26ºC). GsMTx-4 peptide was purchased from Peptides International (Louisville, Kentucky, USA).

Cell culture and transfection

Human embryonic kidney (HEK) 293 cells (ECACC, Salisbury, UK) were grown in medium with 10% FBS and 1% of P/S and plated onto dishes coated with poly-L-lysine for 24-48 h before transfection. A stable HEK-293 line containing a tetracycline-inducible 5ptase IV was grown under conditions described by (Kisseleva *et al.*, 2002). Both types of HEK-293 cells were transfected with the murine TRPC5 (1-2 μg) using Lipofectamine 2000; Invitrogen, Carlsbad, CA; 5 μl/μg DNA) on glass coverslips for 4-6 h. mTRPC5, cloned in the pCI-neo vector (kindly supply by D. Clapham, Harvard Medical School), was co-transfected with green fluorescent protein (GFP; Life Technologies). For specific experiments, rat type 1 histamine receptor (H_1, 0.2 μg/ml; kindly supply by T. Plant, Marburg University) was co-transfected in HEK-293 cells with TRPC5 and GFP. Transfected cells were identified by GFP fluorescence. Induction of 5ptase IV cells was achieved by incubation with tetracycline (0.1 μg/ml for 12-24 h).

Trigeminal ganglion neurones from neonatal mice were cultured as described previously (Viana *et al.*, 2001). In brief, trigeminal ganglia were isolated from anesthetised newborn Swiss OF1 mice (postnatal days 0 to 3), incubated with 1 mg/ml collagenase type IA (Sigma, St. Louis, MO) for 45 min at 37ºC in 5% CO_2 and cultured medium: 45% DMEM, 45% F-12, and 10% fetal bovine serum (Invitrogen), supplemented with 4 mM L-glutamine (Invitrogen), 200 μg/ml streptomycin, 125 μg/ml penicillin, 17 mM glucose, and nerve growth factor (NGF; mouse 7S, 100 ng/ml; Sigma, Sigma, St. Louis, MO). Cells were plated on poly-L-lysine-coated glass coverslips and used 1 day after culture.

Fluorometric calcium measurement

Cells were incubated with 5 μM fura-2AM (Invitrogen) for 45 min at 37ºC in a 5% CO_2 incubator. Recordings were performed in a low-volume chamber with a complete solution exchange of ~1 min. Fluorescence measurements were made with a Zeiss Axioskop FS upright microscope. Fura-2 was excited at 340 nm and 380 nm with a high speed monochromator (TILL Photonics, Germany) and the emitted fluorescence was long-pass filtered at 510 nm. Images were acquired using an Orca ER CCD camera (Hamamatsu Photonics, Japan). Acquisition and analysis were performed with Metafluor software (Molecular Devices Corporation, PA, USA). Cytosolic Ca^{2+} increases are presented as the ratio of the emission intensities of 340 and 380 nm (F_{340}/F_{380}: fluorescence arbitrary units (F.A.U.)). Recordings were made alternately from coverslips with transfected and non-transfected cells. GFP fluorescence was monitored with an excitation wavelength of 470 nm.

The change in cell volume during osmotic swelling was estimated from pairs of Fura-2 fluorescence images recorded at the isosbestic wavelength for Ca^{2+}. The integral fluorescence intensity of an area that contained the whole cell at all times was divided by the integral fluorescence of a small spot within the cell. This fluorescence ratio is reciprocal to the cytosolic Fura-2 concentration and thus reflects the relative change in cell volume (Strotmann *et al.*, 2000).

Electrophysiology

Whole-cell recordings were obtained using 3-5 MΩ borosilicate glass capillary patch pipettes. Current signals were recorded with a Multiclamp 700 amplifier and ramp voltage clamp commands were applied using pCLAMP software and a Digidata 1322A digitizer (Molecular Devices Corporation, Sunnyvale, CA, USA). Cells were held at a potential of –60 mV, and current-voltage (I–V) relations were obtained from voltage ramps from –100 mV to +100 mV with a duration of 400 ms applied every 5s. Current was sampled at a frequency of 20 kHz and filtered at 5 kHz. Series resistance compensation of >50% was used. The internal solution contained (in mM): 135 CsCl, 2 $MgCl_2$, 10 HEPES, 1 EGTA, 5 Na^+2-ATP, pH 7.2 adjusted with CsOH and 300 mOsm/Kg. In some experiments, the pipette solution was modified by adding 10 μM diC_8-PI(4,5)P_2 (Echelon Bioscience, Salt Lake City, UT, USA). The bath solutions for whole-cell recordings were the same as the ones described for the fluorimetric calcium measurements at the bathing solutions and reagents section. In this case, we used a smaller recording chamber with a solution exchange time of ~35 sec.

The pressure-clamp experiments were achieved through the application of controlled pressure steps via the patch-pipette, in whole cell configuration, using a high-speed pressure clamp system (HSPC-1, ALA Scientific Instruments, Westbury, NY; (Besch *et al.*, 2002)).

RT-PCR

Total RNA was isolated from OF-1 adult mice trigeminal ganglia (TG), dorsal root ganglia (DRG), hippocampus and non transfected HEK-293 cells. Animals were terminally anesthetized with CO_2 and the tissues of interest were rapidly removed. Total RNA was extracted from homogenized tissues from 4 animals combining an acid phenol extraction method (TRIzol reagent) and RNeasy mini-columns, (Qiagen, Crawley, UK). 2 μg of total RNA was reverse transcribed using random hexamers and Superscript TM II RT (Invitrogen) in a final volume of 20 μl for 1 hour at 42ºC, followed by 72ºC for 15 min to terminate the reaction. Control reactions for RT-PCR included the absence of the SuperScript II before PCR

and the absence of template which was replaced by water. Control reactions showed no amplification products. 2 µl of the cDNA was added to 18 µl of PCR reaction mixture and the specific primers mTRPC5sense 5'-CTATGAGACCAGAGCTATTGATG-3' and mTRPC5antisense 5'-CTACCAGGGAGATGACGTTGTATG-3' for mouse tissues RNA and hTRPC5sense 5'-TTATGAAACCAGAGCTATCGATG-3' and hTRPC5antisense 5'-CTACCAGGGAGATGACGTTGTATG-3' for human HEK cells RNA.
The cycling protocol used was 3 min at 95ºC, then 30 sec at 95ºC, 20 sec at 60ºC and 30 sec at 72ºC. Reaction samples were separated by standard agarose gel electrophoresis to confirm the specificity and the correct size of the PCR product.

Immunocytochemistry

For TRPC5 immunostaining detection, we used a monoclonal antibody (NeuroMab, UC Davis/NIH, Davis CA, USA). The specificity of the anti-TRPC5 staining was verified in non-transfected HEK-293 cells and in TRPC5-GFP transfected cells (Supplemental Fig. S1). Coverslips with cultured trigeminal neurones and HEK-293 cells were fixed for 10 minutes at room temperature (RT) with 4% paraformaldehyde in PBS. The fixed cells were permeabilised and blocked with 0.1% Triton X-100, 2% goat serum, 1% BSA and 0.05% Tween 20 for 25 minutes and thereafter incubated with the primary antibody against TRPC5 at 1:100 concentration in PBS containing 2% goat serum and 1% BSA for 2 h at RT, then rinsed three times for 2 min at RT and incubated with goat anti-mouse IgG secondary antibody (Sigma, St. Louis, MO) (Alexa fluor 594) at 1:800 concentration. Following thorough wash with PBS, the coverslips were stained with Hoechst (1:1000) and mounted onto slides with Fluoromount-G (Southern Biotech, USA). Cell staining was examined with a laser scanning spectral microscope (Leica TCS SP2 AOBS, Leica Microsystems, Heidelberg, Germany) using a 63x objective with sequential acquisition settings at 1024x1024 pixel resolution. Omission of the primary antibody gave no specific staining and the same laser intensity parameters used for the detection of secondary antibody staining were used to acquire images after incubation with anti-TRPC5. Regions of interest (ROI) were delineated over individual neurones. Neuronal profiles from 12 fields of 3 independent experiments were identified by their characteristic cellular morphology. The fluorescence intensity was represented by 8-bit colour scale (range from 0 to 256 coding intensities). The average value of the non-specific fluorescence intensity was determined in neurones incubated only with the secondary antibody. Those neurones whose mean fluorescence intensity exceeded the average of non-specific fluorescence intensity plus twice its standard deviation were counted as

positive. The analysis of labelled neurones was made using the Leica confocal software and the NIH ImageJ software (Rasband, 2007). Final brightness and contrast were adjusted with Photoshop CS2 (Adobe Systems, USA).

Data analysis

Data were analyzed with WinASCD software (G. Droogmans, KULeuven, Belgium) and Origin 7.5 (OriginLab Corporation, Northampton, MA, USA). When comparing mean amplitude of current increments, we assigned a zero value to non-responding cells for treated and non-treated cells. All data are expressed as means (± SEM). Statistical tests included one-way analysis of variance (ANOVA), the Z-test for comparing proportions and Student's t-test, as indicated. Differences were regarded as statistically significant (*) for $P < 0.05$, (**) for $P < 0.01$ and (***) for $P < 0.001$.

RESULTS

TRPC5 is activated by hypoosmotic-induced cell swelling. We used fura-2 calcium imaging to evaluate the response of HEK-293 cells co-transfected with murine TRPC5 and green fluorescent protein (GFP) (Fig. 1A) to extracellular perfusion with a hypoosmotic solution (210 mOsm) (Fig. 1C). Transient exposure for 4 minutes to a 210 mOsm solution induced a reversible increase in $[Ca^{2+}]_i$ levels in ~25% of GFP positive cells (Fig. 1C,1D,1F). The image 1C corresponds to the time course of calcium increase indicated by the arrow in figure 1D. In the presence of 2.4 mM extracellular Ca^{2+}, hypoosmotically-evoked responses were transient and variable from cell to cell, with a delay ranging from 2-4 min after external medium change and with a delay of 72 ± 14 sec (n= 20 cells) measured from the onset of the volume change produced by the hypoosmotic challenge. Supplemental Fig S2. shows the time course of the relative cell volume increase and the $[Ca^{2+}]_i$ response recorded simultaneously in the same cells, indicating the individual differences in the latency of responses after hypoosmotic change. Responses in GFP(–) cells to hypoosmotic stimuli were minimal (Fig. 1E, F; n= 1555) and undistinguishable from mock transfected cells (i.e. cells co-transfected with the empty vector and GFP; Fig 1F, n=156). The rise in $[Ca^{2+}]_i$ in responding cells averaged 0.25 ± 0.04 (n = 527) fluorescence arbitrary units (F.A.U.) and was entirely attributable to calcium flow across the plasma membrane because it was abolished when we replaced Ca^{2+} in the superfusion medium with 5 mM EGTA (Fig. 1F; n = 195). We investigated further the possibility that Ca^{2+} released from intracellular stores contributes to

the hypoosmotic-induced $[Ca^{2+}]_i$ increases by depletion of the intracellular stores. The bar histogram in Fig. 1G summarised the effect of incubating the cells with 2 μM thapsigargin, an inhibitor of the endoplasmic reticulum Ca^{2+}-ATPase (Thastrup *et al.*, 1990), for 1 h. The depletion of intracellular calcium stores affected neither the percentage of responses of TRPC5 (+) (Fig. 1G) nor the amplitude of the responses (0.35 ± 0.03 F.A.U; n = 307) to hypoosmotic stimulus in the presence of extracellular calcium compared with the responses of cells incubated with 2 μM DMSO, the vehicle of thapsigargin (0.35 ±0.04 F.A.U; n= 169). In contrast, carbachol (Cch) induced Ca^{2+} release was almost abolished in thapsigargin-treated cells (Fig. 1G). These results demonstrate that the hypoosmotic-evoked $[Ca^{2+}]_i$ increase in TRPC5 (+) cells is due to influx of extracellular calcium through activated TRPC5 channels.
Next, we studied the sensitivity of the channel to stimuli of different intensities by testing the effect of extracellular solutions with decreasing osmolarities (260, 210 and 170 mOsm/Kg) on $[Ca^{2+}]_i$ responses in TRPC5-transfected cells. A representative example is shown in the traces of Fig. 2A. The main effect of graded decreases in osmolarity was an increase in the percentage of cells responding to each stimulus (Fig. 2B). In contrast, the amplitude of the responses varied from cell to cell but was similar for the three stimuli (Fig. 2C).
To rule out the possibility that the more frequent response to 170 mOsm solution is due to sensitisation of the cells from two previous applications of hypoosmotic stimulus, we analysed, in a different set of experiments, the responses of cells to applications of a single hypoosomotic stimulus of variable strength. In this case, the percentage of cells responding to 260 and 210 mOsm/kg are half (20% and 23% respectively) of the percentage of cells that respond at 170 mOsm/kg (56%) (Fig. 2E). This result is similar to what was found when all 3 stimuli were applied consecutively which suggest that there is no significant sensitisation or desensitisation after consecutive stimulation (Fig. 2B). Again, when a single hypoosmotic stimulus is applied, no clear trend was observed between the strength of the osmotic stimulus and the increase in fluorescence in the responsive cells (Fig 2F).

Hypooosmotic solution activates TRPC5 channels

To demonstrate that the osmotic stimuli activate membrane TRPC5 channels, we measured whole-cell ionic currents in response to application of hypoosmotic solutions in cells co-transfected with TRPC5 and GFP. As shown in Fig. 3A for a typical experiment, application of a hypoosmotic stimulus induced a large, slowly reversible whole-cell current. Fig. 3B shows, for the same cell, the I–V relationship of the ramp current evoked in control solution and at the peak of the response to hypoosmotic stimulation. The current displays the

characteristic doubly rectifying shape of TRPC5-mediated currents (Schaefer *et al.*, 2000;Strubing *et al.*, 2001). The reversal potential of the osmotically-activated current averaged –8.3 ± 0.6 mV (n=36). Currents were recorded in TRPC5(+) cells with a mean amplitude of –0.276 ± 0.075 nA at –80 mV and 0.564 ± 0.137 nA at +80 mV (Fig 3C, n= 67). The delay between the application of the hypoosmotic stimulus and the onset of the response was 119 ± 16 s, comparable to delays measured during calcium imaging experiments. In contrast, hypoosmotical stimulation did not activate currents with the characteristic TRPC5 signature in cells transfected with the empty vector pCI-Neo (data not shown; n=5) indicating that HEK293 cells lack TRPC5-like endogenous currents. This is in good agreement with the results of (Obukhov & Nowycky, 2008).

Removal of calcium from the extracellular solution prevented the hypoosmotic-activated TRPC5 current, which recovered after adding calcium to the extracellular medium (Fig. 3D). Fig. 3E shows the I–V relation of the whole-cell current at the peak of the response in control solution, in the absence of and after adding calcium (colour points in Fig. 3D). In nominally Ca^{2+}-free external solution with 10 mM EGTA in the pipette, hypoosmotic stimuli did not activate TRPC5-like currents (n=14; Fig. 3F). Even with 1mM EGTA in the pipette, responses were abrogated (only 1 out of 23 TRPC5(+) recorded cells responded to hypoosmotic stimulus; Fig. 3F). These results show that intracellular Ca^{2+} chelation hampers osmotic activation of TRPC5, a result in agreement with activation of TRPC5 by stimulation of G-protein-coupled receptors (Okada *et al.*, 1998; Plant & Schaefer, 2003).

Specific blockade of stretch-activated channels inhibits hypoosmotic-induced TRPC5 activation.

GsMTx-4 is a tarantula peptide having potent blocking actions on stretch-activated channels (Suchyna *et al.*, 2000; Hamill, 2006). Thus, we measured TRPC5-dependent currents during hypoosmotic stimulation in GsMTx-4-treated cells. As shown in Fig. 4A, 5 μM GsMTx-4 strongly reduced TRPC5 currents during hypoosmotic stimulation. The inhibition was reversible upon wash and a typical TRPC5-dependent current was obtained during application of a second hypoosmotic stimulus. The I–V relationship at maximal activation for hypoosmotic stimulation in the presence and after wash of GsMTx-4 is represented in Fig. 4C. All the recorded TRPC5 (+) cells responded to hypoosmotic stimulation (n=10; Fig. 4E) with an average increase of 0.324 ± 0.09 nA at -80 mV and 0.431 ± 0.128 nA at +80 mV (Fig. 4F), however only 1 of the 8 cells treated with GsMTx-4 responded to the hypoosmotic stimulation at -80 mV and 3 of 8 cells at +80 mV (in average, 0.006 nA at -80 mV and 0.05 ±

0.03 nA at +80 mV; Fig. 4E-F). The block of hypoosmotically-induced current activation was more effective on the inward component of the current (Fig. 4C), consistent with a block occurring at the extracellular side (Suchyna *et al.*, 2004). These results argue that the toxin blocks the activation of TRPC5 by osmotic-induced membrane stretch.

TRPC5 channels are known to activate following stimulation of G-protein coupled-receptors of the $G_{q/11}$ family which couple to phospholipase C_β (PLC_β) (Plant & Schaefer, 2005; Beech, 2007). Co-transfection of TRPC5 and type 1 histamine $(H_1)_1$ receptors has been used by some authors chracterizing activation of TRPC5 (Schaefer *et al.*, 2000; Jung *et al.*, 2003; Obukhov & Nowycky, 2004; Obukhov & Nowycky, 2008). Indeed, histamine application evoked large, consistent inward and outward currents in TRPC5 transfected cells. Therefore, we also studied current activation to hypoosmotic solution in GsMTx-4-treated cells co-transfected with TRPC5 and H_1 receptors, a canonical Gq/11-coupled receptor. Interestingly, H_1-mediated activation of TRPC5 was also affected by the toxin. The activation of the current evoked by 100 μM histamine was potently and reversibly blocked in the presence of GsMTx-4 (Fig. 4B). The residual current had a much slower rise time and the peptide reduced the current amplitude significantly; only 3 of the 10 recorded cells responded to 100 μM histamine (Fig. 4E). Figure 4D shows the typical double rectified I–V relationship of the TRPC5 current activated after removal of the toxin. The amplitude of the current activated by 100 μM histamine was almost fully blocked by the toxin at negative potentials (it diminished from 1.34 ± .235 nA to 0.07 ± 0.05 nA at -80 mV) and was also strongly reduced at positive potentials (from 1.7 ± 0.3 nA to 0.15 ± 0.11 nA at +80 mV (n=10); Fig. 4F). All together these results indicated that TRPC5 channels are blocked by a toxin having effects on stretch-activated channels.

Phospholipase activity is not required for osmotic activation of TRPC5

Next, we tried to dissect the signalling pathway involved in the hypoosmotic activation of TRPC5 channels. We asked whether phospholipase C (PLC), the canonical mechanism for receptor-mediated activation of TRPC5 (Schaefer *et al.*, 2000; Putney, Jr., 2004) is involved. To this end, we tested the PLC inhibitor U-73122 in cells transfected with TRPC5. As shown in the representative trace of Fig.5A, treating cells with 5 μM U-73122 did not prevent activation of TRPC5 currents by hypoosmotic solutions. In contrast, U-73122 fully abrogated the response to application of 10 μM Cch that activates endogenous muscarinic Gq-coupled receptors in this clone of HEK-293 cells. Figures 5B and 5C summarise these results. After

incubation with U-73122, all recorded cells (n = 6) responded to hypoosmotic stimulation (Fig. 5B) with an average current increase identical to that of non treated cells (0.221 ± 0.09 nA at -80 mV and 0.531 ± 0.24 nA at +80 mV in treated cells versus 0.212 ± 0.17 nA at -80 mV and 0.526 ± 0.366 nA at +80 mV in control cells; n = 8, Fig. 5C). On the other hand, only 1 of 6 cell (Fig.5B) responded to 10 μM Cch after U-73122 incubation with a average current increase of 0.016 ± 0.014 nA at -80 mV and 0.036 ± 0.005 nA at +80 mV (Fig. 5C) whereas all cells responded to Cch in control conditions (0.385 ± 0.197 nA at -80 mV and 0.603 ± 0.211 nA at +80 mV; n=12, Fig. 5C). Incubation with U-73343, an inactive analogue with little or no effect on PLC activity, did not affect the activation of TRPC5 channels, neither by hypoosmotic solution (n=8) nor by Cch (n=8). From these results it is clear that the activation of TRPC5 by hypoosmotic solution is not attributable to osmotic activation of PLC (Osol *et al.*, 1993).

Cell swelling can also activate phospholipase A2 (PLA_2) (Pedersen *et al.*, 2000) and the osmotic activation of the TRPV4 channel is thought to be secondary to PLA_2-dependent synthesis of AA (arachidonic acid), which is then metabolized to 5'-6' EET (Vriens *et al.*, 2004). We used N-(p-amyl-cinnamoyl)anthranilic acid (ACA), a potent inhibitor of PLA_2, to test the involvement of this enzyme in the osmotic activation of TRPC5. As shown in Fig. 5D, pre-incubation with 20 μM ACA did not prevent $[Ca^{2+}]_i$ increases (0.32 ± 0.025 F.A.U. n = 74 in 4 independent experiments) evoked by hypoosmotic stimulation. Figure 5E shows the typical TRPC5-mediated whole-cell current, during 210 mOsm stimulation, in a cell pre-incubated with 20 μM ACA: 3 out of 4 cells responded to ACA with mean current amplitude of 0.369 ± 0.216 nA at -80 mV and 0.533 ± 0.250 nA at +80 mV. This amplitude is similar to that obtained in untreated TRPC5(+) cells. Figure 5F shows, in the same cell, the I–V relationship of the ramp current in control solution and at the peak of the response to hypoosmotic stimulation in the presence of ACA. As a matter of fact, an increase in the current was consistently observed after application of ACA (Fig. 5F) (Kraft *et al.*, 2006).

Activation of TRPC5 by hypoosmotic stimuli depends of intracellular PIP_2 levels.

Stimulation of phospholipase C-activating receptors cause hydrolysis of the membrane trace lipid phosphatidylinositol 4,5-bisphosphate (PIP_2). Recent studies have highlighted the important role of PIP_2 in the gating of many ion channels (Suh & Hille, 2005; Gamper & Shapiro, 2007) particularly TRP channels (reviewed by Qin, 2007). Therefore, we tested whether PIP_2 could be involved in the activation of TRPC5 channels by osmotic stretch. To

this end, we transfected TRPC5 into a HEK293 cell line stably expressing, under tetracycline control, a phosphoinositide-specific inositol polyphosphate 5-phosphatase IV (5ptase IV). In this cellular system, induction of 5ptase IV caused an 8- to 15-fold depletion of PIP_2 levels (Kisseleva *et al.*, 2002). As shown in Fig. 6A, B in non-induced cells, labelled tet(-), hypoosmotic solutions evoked robust TRPC5 currents. Figures 6F-G summarise the percentage of cells that responded to different experimental conditions and the averaged amplitude of the responses, respectively. 14 out of 17 cells responded to hypoosmotic solution (0.381 ± 0.121 nA at -80 mV and 0.550 ± 0.152 nA at +80 mV) in control conditions. In contrast, in PIP_2-depleted cells, labelled tet(+), the responses to hypoosmotic stimuli was significantly reduced and was observed in only 5 of 26 cells (Fig. 6F). Furthermore, the amplitude of the current activated by hypoosmotic stimuli was strongly and significantly reduced (measuring on average 0.022 ± 0.019 nA at -80 mV and 0.0085 ± 0.061 nA at +80 mV). As an additional control for PIP_2 depletion, we analysed the activation of the TRPC5 channels following stimulation of G-protein coupled-receptors via activation of the endogenous P2Y receptors expressed in this particular cell line (Chen *et al.*, 2006). In 16 of the 17 untreated TRPC5(+) cells tested, application of 500 μM ATP activated a robust TRPC5-like current (on average 0.680 ± 0.155 nA at -80 mV and 0.757 ± 180 nA at +80 mV; Fig 6A, B, F, G). In contrast, in PIP_2-depleted cells, the responses to ATP were strongly reduced and only 8 of 26 cells were activated by ATP (in average 0.021 ± 0.009 nA at -80 mV and 0.071 ± 0.035 nA at +80 mV; Fig. 6C, D). If PIP_2 underlies the hypoosmotic- and ATP mediated current activation, the application of exogenous PIP_2 to PIP_2-depleted cells should lead to current recovery. We added diC_{8}-PIP_2, a water-soluble form of PIP_2, to the intracellular patch pipette solution and were able to recover the hypoosmotic activated current in 6 of 10 tet(+) cells, a percentage of responses similar to the one found in tet(-) cells. The current amplitude also increased modestly, without reaching the significance levels (in average, 0.067 ± 0.022 nA at -80 mV and 0.202 ± 0.095 nA at +80 mV; Fig. 6G). In contrast, the responses to ATP were only recovered in 3 of the 10 cells tested (data not shown).
We also tested the role of PIP_2 in the increases of $[Ca^{2+}]_i$ evoked by hypoosmotic stimulation of cells transfected with TRPC5. Hypoosmotic stimulation of control (i.e. non-induced) cells, elevated $[Ca^{2+}]_i$ in 18% of the TRPC5(+) cells (Fig. 6H, J) with an increase of 0.25 ± 0.19 F.A.U. (60 of 328 cells in three independent experiments). The cells also responded to 500 μM ATP (0.96 ± 0.17 F.A.U.; 284 of 289 cells from 8 independent experiments; Fig. 6H, J). After induction of the 5ptase IV, the response to hypoosmotic solution was fully abrogated (n=114), while the response to ATP was strongly reduced (19.3%, n=114; Fig. 6I, J). The

mean calcium increase of the ATP-responding cells also decreased to 0.5 ± 0.1 F.A.U. Overall, these data indicate that basal membrane PIP_2 levels are required for hypoosmotic and agonist-mediated activation of TRPC5 channels.

Membrane stretch induced by pressure activates the TRPC5 channel

Gating of mechano-sensitive cation channels has been studied in the whole-cell configuration by applying positive pressure through the patch pipette (Hamill & McBride, Jr., 1997). Such manipulations increase the cell volume and exert membrane stretch in much the same way as hypotonic solutions. The significant difference with hypotonic swelling, however, is that pressure-induced inflation occurs without altering the cytosolic concentrations of ions, as occurs during hypotonic swelling. Using a fast pressure-clamp technique (Bessac & Fleig, 2007), we studied the pressure-induced activation of the TRPC5 channel. We kept TRPC5 transfected cells in the standard external and internal (patch pipette) solutions. Membrane stretch was induced by positive pressure applied to the patch pipette. Application of repeated positive pressure pulses of increasing amplitude from 10 to 140 mmHg activated a doubly rectifying current in TRPC5(+) cells (Fig. 7A-B). Figure 7A shows the whole-cell current induced by positive pressure at -80 and +80 mV. The channel was activated when the pressure reached an average threshold of 21.3 ± 2.7 mm of Hg in 16 of the 19 recorded cells, with an average increment in current of 0.497 ± 0.116 nA at -80 mV and 1.58 ± 0.22 nA at + 80 mV (n= 19 cells; Fig. 7C). Following a variable delay after pressure application, the onset of current activation was 22 ± 5.6 s which is considerable shorter than delays measured during hypoosmotic-current activation. Upon removal of the intracellular positive pressure, the current slowly declined to basal levels. The reversal potential of the stretch-activated current was close to zero (-0.3 ± 0.6 mV; n = 16). Figure 7B shows, in the same cell, the I–V relationship of the ramp current in control solution and at the peak of the response to pressure stimulation (30 mm Hg in this case).

In some experiments we were able to apply consecutively both stimuli, i.e. hypoosmotic solution followed by positive pressure, to the same cell. All TRPC5(+) cells tested (n=5) responded to both stimuli without statistically significant differences in current amplitude (Fig.7D-E). As occurred with hypoosmotic stimulation, positive pressure application did not activate currents with the characteristic TRPC5 signature in cells transfected with the empty vector pCI-neo (Fig. 7F; n=11).

TRPC5 channel is expressed in mouse primary sensory neurones

We used specific primers for mouse TRPC5 to determine the expression of the channel in TG and DRG ganglia and in hippocampus. Our RT-PCR analysis showed that TRPC5 was expressed in the tested tissues (Fig. 8A). Next, we examined TRPC5 protein expression in mouse ganglia using immunocytochemical staining. TRPC5 was detected in 62% of all TG neurones (n= 295 from 12 different fields, from 3 experiments). Figure 8 show representative images of TG cultured cells under visible illumination (B) and the fluorescence image after labelling with an antibody against TRPC5 (C). Figure (D-E) shows the lack of labelling when omitting the primary antibody. The histogram of figure 8F shows the size distribution plots of neurones expressing and not expressing TRPC5, with average sizes of $110 \pm 4\ \mu m^2$ (n=183) and $111 \pm 6\ \mu m^2$ (n= 112) respectively.

DISCUSSION

Mechano-detection is essential for many physiological processes like touch, hearing and blood pressure control. Nonetheless, the molecular identity of ion channels sensing mechanical forces in tissues remains uncertain (Christensen & Corey, 2007; Venkatachalam & Montell, 2007; Lumpkin & Caterina, 2007). Moreover, how mechanical deformation of the cell membrane translates into channel activity is not firmly established. Genetic studies in *C. elegans* and fruit flies support the involvement of TRP channels in mechanotransduction (Colbert *et al.*, 1997; Christensen & Corey, 2007; Kahn-Kirby & Bargmann, 2006). In mammals there is also fragmentary evidence supporting a role for TRP channels in mechano- and osmodetection (reviewed by Pedersen & Nilius, 2007). Thus, TRPV4 channels contribute to activation of high-threshold cutaneous mechanoreceptors (Suzuki *et al.*, 2003; Alessandri-Haber *et al.*, 2004), hypothalamic osmoregulation (Liedtke & Friedman, 2003; Liedtke, 2007; Bourque, 2008), and bladder voiding responses (Gevaert *et al.*, 2007). Also, several TRPs, including TRPC1, TRPC3, TRPC6, TPV2 and TRPM4 have been implicated in the regulation of myogenic vascular tone (Beech, 2005; Christensen & Corey, 2007).

Our study shows that TRPC5, a widely expressed ion channel in mammalian tissues, is activated by swelling and pressure-induced membrane stretch. The TRPC5 current activated by hypoosmotic stimulation is dependent on extracellular Ca^{2+}. Furthermore, current activation is also prevented by intracellular Ca^{2+} buffering, suggesting that Ca^{2+} elevation and basal Ca^{2+} levels are needed to sustain activation of the channel. These findings agree with the receptor-mediated activation of TRPC5 which is also strongly dependent on $[Ca^{2+}]_i$ elevation (Schaefer *et al.*, 2000). A channel that is calcium permeable and calcium-activated represents

a typical example of a positive feedback mechanism. Thus, calcium influx induced by membrane stretch may explain the variability in the responses and the lack of a clear relation between stimulus strength and current amplitude. Moreover, membrane stretch induced by application of positive pressure through the patch pipette, also activated TRPC5 channels, suggesting that their gating is closely related to membrane tension rather than being secondary to changes in intracellular signalling factors.

The blocking effect of GsMTx-4, a specific modifier of nonselective mechanosensitive channels (Suchyna *et al.*, 2000; Park *et al.*, 2008) further supports the tenet that TRPC5 could acts as a membrane stretch transducer. Our data concur with the model proposed by Spassova et al, (2006) to explain the inhibition of TRPC6 channels by GsMTx-4. In control conditions, hypoosmotic stimulation leads to cell swelling and membrane stretch. These forces are transmitted through the lipid bilayer to gate the channel into the open state. Insertion of GsMTx-4 in the outer leaflet of the membrane relieves the lipid stress leading to channel closure. GsMTx-4 also inhibits the activation of TRPC5 by receptor stimulation which favours the idea that the toxin is blocking the channel and it is not acting on a possible mechanosensitive element upstream of TRPC5 activation. According to the model, activation of PLC-coupled receptors produces a breakdown of the charged PIP_2 molecules to form the uncharged DAG. This change in lipid geometry produces stress and/or exposure of channel residues and opening. As occurs with stretch-activation, GsMTx-4 inserts in the bilayer and relieves lipid stress. Although neither DAG nor arachidonic acid or other fatty acids activate TRPC5 (Schaefer *et al.*, 2000), PLC metabolizes other membrane phospholipids that could modify the structure of the membrane. Thus, the toxin could inhibit the activation by a similar mechanism as for the direct stretch activation. Moreover, we showed that PLA_2 that is activated by cell swelling and mediates the osmotic activation of TRPV4 (Vriens *et al.*, 2004), is not involved in the osmotic activation of TRPC5. Finally, our results also show that the osmotic activation of TRPC5 was still observed in the presence of the PLC inhibitor U-73122 indicating that TRPC5 channels are activated by hypoosmotic membrane stretch through a PLC-independent mechanism.

PIP_2 is emerging as a critical modulator of many TRP channels (Qin, 2007; Lukacs *et al.*, 2007; Brauchi *et al.*, 2007). Ours results clearly show that PIP_2 is necessary for both, hypoosmotic activation and PLC-coupled receptor activation of the TRPC5 channel. Furthermore, reintroducing a water-soluble PIP_2 analog in the cell recovered the response to mechanical and receptor-mediated activation, suggesting that the role of PIP_2 is upstream of both signalling pathways, perhaps intimately linked to the gating of the channel itself. By

analogy with previous work, it could be speculated that electrostatic interactions between PIP_2 and positively charged intracellular residues of the channel lead to stabilization of the open state (Suh & Hille, 2005; Gamper & Shapiro, 2007; Voets & Nilius, 2007). More complex scenarios involving indirect interactions between PIP_2 and TRPC5 are also possible. The recruitment of new TRPC5 channels to the plasma membrane by epidermal growth factor is also dependent on PIP_2 (Bezzerides *et al.*, 2004). However, the fact that PIP_2 is required for the activation of TRPC5 by the hypoosmotic stimulus seems at odds with a receptor-mediated activation of TRPC5 that should lead to PLC activation and decreased membrane PIP_2 levels. The apparent bell-shaped relationship between membrane PIP_2 levels and TRPC5 activity resembles the dependence of IP_3 receptors on Ca^{2+} levels (Bezprozvanny *et al.*, 1991). Another possibility to consider is the affinity of TRPC5 for PIP_2. For channels with apparent high affinity for PIP_2, a moderate depletion of PIP_2 (as could be the case for the depletion of PIP_2 after PLC-coupled receptor activation) would not inhibit activity (Rohacs, 2007). In contrast, a more severe depletion would hamper the gating of the channel. Other hypothetical explanations for this conundrum follow. Activation of TRPC5 following PLC stimulation may depend on other, yet unidentified, signalling molecule. Distinct pools of PIP_2 molecules with differential accessibility to PLC may exist as well (Lukacs *et al.*, 2007). This dual role of PIP_2 on gating has been observed in TRPC6 channels in mesenteric artery myocytes. In this case, PIP_2 is a precursor for DAG production for channel activation and a direct inhibitor of the ion channel (Albert *et al.*, 2008). Recent work (Trebak *et al.*, 2008) also supports the complex regulation of TRPC5 by PIP2, proposing that polyphosphoinositides may have at least two distinct functions in regulating TRPC5 channel activity.

Mechanically sensitive channels that are gated directly by the mechanical stimulus are expected to respond with delays in the order of ms (Christensen & Corey, 2007). Our observed delays for TRPC5, in the range of seconds, suggest that the activation mechanism is indirect. It could involve activation of second messenger cascades or phosphorylation/dephosphorylation mechanism (Pedersen & Nilius, 2007; Lewin, 2008). However, it is possible that TRPC5 is part of a multi-protein complex in vivo and the observed delays reflect a poor coupling efficiency between the channel and the force sensing mechanism. Investigations on genetically modified mice may provide clues about these various possibilities.

TRPC5 is highly expressed in the frontal cortex, hypothalamus, hippocampus and visceral sensory neurones (Philipp *et al.*, 1998; Riccio *et al.*, 2002; Greka *et al.*, 2003; Glazebrook *et al.*, 2005; Fowler *et al.*, 2007). Still, little is known about its possible role in sensory

transduction. Using RT-PCR and inmunocytochemistry we show the presence of TRPC5 in trigeminal sensory neurones, thus extending previous data about the expression of TRPC5 in neurones of the hippocampus and DRG (Philipp *et al.*, 1998; Greka *et al.*, 2003; Wu *et al.*, 2008). Neurones expressing TRPC5 in the trigeminal ganglion were mainly of small diameter. Most of the small neurones in sensory ganglia are nociceptive, and respond to noxious mechanical forces, either exclusively (high threshold mechanosensitive neurones) or combined with other transduction capacities (polymodal nociceptor neurones) (Felipe *et al.*, 1999; Chen *et al.*, 1995). Therefore, the possibility that TRPC5 expression is associated with the mechanosensitive properties of nociceptive neurones must be considered. At least three distinct types of mechanosensitive channels have been identified, contributing to the transduction of mechanical forces by primary sensory neurones, each with different pressure thresholds and biophysical properties (Cho *et al.*, 2002; Hu & Lewin, 2006). Their molecular identity remains unknown. Another TRP channel expressed by cutaneous sensory neurones, TRPV4, is also activated by osmotic swelling and participates in high threshold mechanical responses (Suzuki *et al.*, 2003; Alessandri-Haber *et al.*, 2004). Large local changes in tonicity occur in the skin during pain-enhancing inflammatory conditions *in vivo* (Cao *et al.*, 2000; Liu *et al.*, 2007). Moreover, Liu *et al.* (2007), have shown recently that changes in osmolarity sensitise TRPV1-mediated capsaicin responses in trigeminal ganglion. We showed a marked block of TRPC5 by GsMTx-4. Interestingly, this toxin, reduced mechanically evoked pain-like behaviour in rats (Park *et al.*, 2008).

A possible function of TRPC5 as a mechano-osmotic transducer also correlates well with its expression pattern in tissues that are subjected to strong hydrostatic forces, like vascular and gastric smooth muscle and renal podocites. Recent studies in TRPC1(-/-) and TRPC6(-/-) mice suggests that, contrary to previous claims, TRPC1 and TRPC6 are not an obligatory component of stretch-activated ion channel complexes in vascular smooth muscle cells (Dietrich *et al.*, 2007; Gottlieb *et al.*, 2008; Sharif-Naeini *et al.*, 2008). It is known that TRPC channels can form functional heteromeric complexes (Hofmann *et al.*, 2002; Strubing *et al.*, 2001). In light of our findings, we propose that heteromeric assemblies of TRPC5 with other TRPC subunits may have mechanosensitive properties. In this case, elimination of a single subunit may be compensated by the formation of homeomeric complexes retaining mechanosensitivity. Further studies in TRPC5 k.o mice and double mutants should clarify their physiological role in mechano-transduction and osmotic regulation. In the meantime, caution is needed before ascribing a definitive role to TRPC channels in physiological transduction of mechanical forces.

REFERENCES

Albert AP, Saleh SN, & Large WA (2008). Inhibition of native TRPC6 channel activity by phosphatidylinositol 4,5-bisphosphate in mesenteric artery myocytes. *J Physiol* **586**, 3087-3095.

Alessandri-Haber N, Dina OA, Yeh JJ, Parada CA, Reichling DB, & Levine JD (2004). Transient receptor potential vanilloid 4 is essential in chemotherapy-induced neuropathic pain in the rat. *J Neurosci* **24**, 4444-4452.

Beech DJ (2005). Emerging functions of 10 types of TRP cationic channel in vascular smooth muscle. *Clin Exp Pharmacol Physiol* **32**, 597-603.

Beech DJ (2007). Canonical transient receptor potential 5. *Handb Exp Pharmacol* 109-123.

Beech DJ, Muraki K, & Flemming R (2004). Non-selective cationic channels of smooth muscle and the mammalian homologues of Drosophila TRP. *J Physiol* **559**, 685-706.

Besch SR, Suchyna T, & Sachs F (2002). High-speed pressure clamp. *Pflugers Arch* **445**, 161-166.

Bessac BF & Fleig A (2007). TRPM7 channel is sensitive to osmotic gradients in human kidney cells. *J Physiol* **582**, 1073-1086.

Bezprozvanny I, Watras J, & Ehrlich BE (1991). Bell-shaped calcium-response curves of Ins(1,4,5)P3- and calcium-gated channels from endoplasmic reticulum of cerebellum. *Nature* **351**, 751-754.

Bezzerides VJ, Ramsey IS, Kotecha S, Greka A, & Clapham DE (2004). Rapid vesicular translocation and insertion of TRP channels. *Nat Cell Biol* **6**, 709-720.

Bourque CW (2008). Central mechanisms of osmosensation and systemic osmoregulation. *Nat Rev Neurosci* **9**, 519-531.

Brauchi S, Orta G, Mascayano C, Salazar M, Raddatz N, Urbina H, Rosenmann E, Gonzalez-Nilo F, & Latorre R (2007). Dissection of the components for PIP2 activation and thermosensation in TRP channels. *Proc Natl Acad Sci U S A* **104**, 10246-10251.

Cao T, Pinter E, Al Rashed S, Gerard N, Hoult JR, & Brain SD (2000). Neurokinin-1 receptor agonists are involved in mediating neutrophil accumulation in the inflamed, but not normal, cutaneous microvasculature: an in vivo study using neurokinin-1 receptor knockout mice. *J Immunol* **164**, 5424-5429.

Chen CC, Akopian AN, Sivilotti L, Colquhoun D, Burnstock G, & Wood JN (1995). A P2X purinoceptor expressed by a subset of sensory neurons. *Nature* **377**, 428-431.

Chen X, Talley EM, Patel N, Gomis A, McIntire WE, Dong B, Viana F, Garrison JC, & Bayliss DA (2006). Inhibition of a background potassium channel by Gq protein alpha-subunits. *Proc Natl Acad Sci U S A* **103**, 3422-3427.

Cho H, Shin J, Shin CY, Lee SY, & Oh U (2002). Mechanosensitive ion channels in cultured sensory neurons of neonatal rats. *J Neurosci* **22**, 1238-1247.

Christensen AP & Corey DP (2007). TRP channels in mechanosensation: direct or indirect activation? *Nat Rev Neurosci* **8**, 510-521.

Clapham DE (2003). TRP channels as cellular sensors. *Nature* **426**, 517-524.

Colbert HA, Smith TL, & Bargmann CI (1997). OSM-9, a novel protein with structural similarity to channels, is required for olfaction, mechanosensation, and olfactory adaptation in Caenorhabditis elegans. *J Neurosci* **17**, 8259-8269.

Dhaka A, Viswanath V, & Patapoutian A (2006). Trp ion channels and temperature sensation. *Annu Rev Neurosci* **29**, 135-161.

Dietrich A, Chubanov V, Kalwa H, Rost BR, & Gudermann T (2006). Cation channels of the transient receptor potential superfamily: their role in physiological and pathophysiological processes of smooth muscle cells. *Pharmacol Ther* **112**, 744-760.

Dietrich A, Kalwa H, Storch U, Mederos YS, Salanova B, Pinkenburg O, Dubrovska G, Essin K, Gollasch M, Birnbaumer L, & Gudermann T (2007). Pressure-induced and store-operated cation influx in vascular smooth muscle cells is independent of TRPC1. *Pflugers Arch* **455**, 465-477.

Earley S, Waldron BJ, & Brayden JE (2004). Critical role for transient receptor potential channel TRPM4 in myogenic constriction of cerebral arteries. *Circ Res* **95**, 922-929.

Felipe CD, Gonzalez GG, Gallar J, & Belmonte C (1999). Quantification and immunocytochemical characteristics of trigeminal ganglion neurons projecting to the cornea: effect of corneal wounding. *Eur J Pain* **3**, 31-39.

Flemming PK, Dedman AM, Xu SZ, Li J, Zeng F, Naylor J, Benham CD, Bateson AN, Muraki K, & Beech DJ (2006). Sensing of lysophospholipids by TRPC5 calcium channel. *J Biol Chem* **281**, 4977-4982.

Fowler MA, Sidiropoulou K, Ozkan ED, Phillips CW, & Cooper DC (2007). Corticolimbic expression of TRPC4 and TRPC5 channels in the rodent brain. *PLoS ONE* **2**, e573.

Gamper N & Shapiro MS (2007). Regulation of ion transport proteins by membrane phosphoinositides. *Nat Rev Neurosci* **8**, 921-934.

Gevaert T, Vriens J, Segal A, Everaerts W, Roskams T, Talavera K, Owsianik G, Liedtke W, Daelemans D, Dewachter I, Van Leuven F, Voets T, De Ridder D, & Nilius B (2007). Deletion of the transient receptor potential cation channel TRPV4 impairs murine bladder voiding. *J Clin Invest* **117**, 3453-3462.

Glazebrook PA, Schilling WP, & Kunze DL (2005). TRPC channels as signal transducers. *Pflugers Arch* **451**, 125-130.

Gottlieb P, Folgering J, Maroto R, Raso A, Wood TG, Kurosky A, Bowman C, Bichet D, Patel A, Sachs F, Martinac B, Hamill OP, & Honore E (2008). Revisiting TRPC1 and TRPC6 mechanosensitivity. *Pflugers Arch* **455**, 1097-1103.

Greka A, Navarro B, Oancea E, Duggan A, & Clapham DE (2003). TRPC5 is a regulator of hippocampal neurite length and growth cone morphology. *Nat Neurosci* **6**, 837-845.

Grimm C, Kraft R, Sauerbruch S, Schultz G, & Harteneck C (2003). Molecular and functional characterization of the melastatin-related cation channel TRPM3. *J Biol Chem* **278**, 21493-21501.

Hamill OP (2006). Twenty odd years of stretch-sensitive channels. *Pflugers Arch* **453**, 333-351.

Hamill OP & Martinac B (2001). Molecular basis of mechanotransduction in living cells. *Physiol Rev* **81**, 685-740.

Hamill OP & McBride DW, Jr. (1997). Induced membrane hypo/hyper-mechanosensitivity: a limitation of patch-clamp recording. *Annu Rev Physiol* **59**, 621-631.

Hofmann T, Schaefer M, Schultz G, & Gudermann T (2002). Subunit composition of mammalian transient receptor potential channels in living cells. *Proc Natl Acad Sci U S A* **99**, 7461-7466.

Hu J & Lewin GR (2006). Mechanosensitive currents in the neurites of cultured mouse sensory neurones. *J Physiol* **577**, 815-828.

Inoue R, Jensen LJ, Shi J, Morita H, Nishida M, Honda A, & Ito Y (2006). Transient receptor potential channels in cardiovascular function and disease. *Circ Res* **99**, 119-131.

Jung S, Muhle A, Schaefer M, Strotmann R, Schultz G, & Plant TD (2003). Lanthanides potentiate TRPC5 currents by an action at extracellular sites close to the pore mouth. *J Biol Chem* **278**, 3562-3571.

Kahn-Kirby AH & Bargmann CI (2006). TRP channels in C. elegans. *Annu Rev Physiol* **68**, 719-736.

Kisseleva MV, Cao L, & Majerus PW (2002). Phosphoinositide-specific inositol polyphosphate 5-phosphatase IV inhibits Akt/protein kinase B phosphorylation and leads to apoptotic cell death. *J Biol Chem* **277**, 6266-6272.

Kraft R, Grimm C, Frenzel H, & Harteneck C (2006). Inhibition of TRPM2 cation channels by N-(p-amylcinnamoyl)anthranilic acid. *Br J Pharmacol* **148**, 264-273.

Kraft R & Harteneck C (2005). The mammalian melastatin-related transient receptor potential cation channels: an overview. *Pflugers Arch* **451**, 204-211.

Kung C (2005). A possible unifying principle for mechanosensation. *Nature* **436**, 647-654.

Lemarechal H, Anract P, Beaudeux JL, Bonnefont-Rousselot D, Ekindjian OG, & Borderie D (2007). Impairment of thioredoxin reductase activity by oxidative stress in human rheumatoid synoviocytes. *Free Radic Res* **41**, 688-698.

Lewin GR (2008). Stretching it for pain. *Pain* **137**, 3-4.

Liedtke W (2007). Role of TRPV ion channels in sensory transduction of osmotic stimuli in mammals. *Exp Physiol* **92**, 507-512.

Liedtke W, Choe Y, Marti-Renom MA, Bell AM, Denis CS, Sali A, Hudspeth AJ, Friedman JM, & Heller S (2000). Vanilloid receptor-related osmotically activated channel (VR-OAC), a candidate vertebrate osmoreceptor. *Cell* **103**, 525-535.

Liedtke W & Friedman JM (2003). Abnormal osmotic regulation in trpv4-/- mice. *Proc Natl Acad Sci U S A* **100**, 13698-13703.

Liu L, Chen L, Liedtke W, & Simon SA (2007). Changes in osmolality sensitize the response to capsaicin in trigeminal sensory neurons. *J Neurophysiol* **97**, 2001-2015.

Lukacs V, Thyagarajan B, Varnai P, Balla A, Balla T, & Rohacs T (2007). Dual regulation of TRPV1 by phosphoinositides. *J Neurosci* **27**, 7070-7080.

Lumpkin EA & Caterina MJ (2007). Mechanisms of sensory transduction in the skin. *Nature* **445**, 858-865.

Maroto R, Raso A, Wood TG, Kurosky A, Martinac B, & Hamill OP (2005). TRPC1 forms the stretch-activated cation channel in vertebrate cells. *Nat Cell Biol* **7**, 179-185.

Maurice MM, Nakamura H, Gringhuis S, Okamoto T, Yoshida S, Kullmann F, Lechner S, van d, V, Leow A, Versendaal J, Muller-Ladner U, Yodoi J, Tak PP, Breedveld FC, & Verweij CL (1999). Expression of the thioredoxin-thioredoxin reductase system in the inflamed joints of patients with rheumatoid arthritis. *Arthritis Rheum* **42**, 2430-2439.

Muraki K, Iwata Y, Katanosaka Y, Ito T, Ohya S, Shigekawa M, & Imaizumi Y (2003). TRPV2 is a component of osmotically sensitive cation channels in murine aortic myocytes. *Circ Res* **93**, 829-838.

Obukhov AG & Nowycky MC (2004). TRPC5 activation kinetics are modulated by the scaffolding protein ezrin/radixin/moesin-binding phosphoprotein-50 (EBP50). *J Cell Physiol* **201**, 227-235.

Obukhov AG & Nowycky MC (2008). TRPC5 channels undergo changes in gating properties during the activation-deactivation cycle. *J Cell Physiol* **216**, 162-171.

Okada T, Shimizu S, Wakamori M, Maeda A, Kurosaki T, Takada N, Imoto K, & Mori Y (1998). Molecular cloning and functional characterization of a novel receptor-activated TRP Ca2+ channel from mouse brain. *J Biol Chem* **273**, 10279-10287.

Osol G, Laher I, & Kelley M (1993). Myogenic tone is coupled to phospholipase C and G protein activation in small cerebral arteries. *Am J Physiol* **265**, H415-H420.

Park SP, Kim BM, Koo JY, Cho H, Lee CH, Kim M, Na HS, & Oh U (2008). A tarantula spider toxin, GsMTx4, reduces mechanical and neuropathic pain. *Pain* **137**, 208-217.

Pedersen S, Lambert IH, Thoroed SM, & Hoffmann EK (2000). Hypotonic cell swelling induces translocation of the alpha isoform of cytosolic phospholipase A2 but not the gamma isoform in Ehrlich ascites tumor cells. *Eur J Biochem* **267**, 5531-5539.

Pedersen SF & Nilius B (2007). Transient receptor potential channels in mechanosensing and cell volume regulation. *Methods Enzymol* **428**, 183-207.

Philipp S, Hambrecht J, Braslavski L, Schroth G, Freichel M, Murakami M, Cavalie A, & Flockerzi V (1998). A novel capacitative calcium entry channel expressed in excitable cells. *EMBO J* **17**, 4274-4282.

Plant TD & Schaefer M (2003). TRPC4 and TRPC5: receptor-operated Ca2+-permeable nonselective cation channels. *Cell Calcium* **33**, 441-450.

Plant TD & Schaefer M (2005). Receptor-operated cation channels formed by TRPC4 and TRPC5. *Naunyn Schmiedebergs Arch Pharmacol* **371**, 266-276.

Putney JW, Jr. (2004). The enigmatic TRPCs: multifunctional cation channels. *Trends Cell Biol* **14**, 282-286.

Qin F (2007). Regulation of TRP ion channels by phosphatidylinositol-4,5-bisphosphate. *Handb Exp Pharmacol* 509-525.

Raoux M, Rodat-Despoix L, Azorin N, Giamarchi A, Hao J, Maingret F, Crest M, Coste B, & Delmas P (2007). Mechanosensor channels in mammalian somatosensory neurons. *Sensors* **7**, 1667-1682.

Rasband W (2007). Image J. *ImageJ, U S National Institutes of Health, Bethesda, Maryland, USA, http://rsb info nih gov/ij/, 1997-2005*.

Riccio A, Medhurst AD, Mattei C, Kelsell RE, Calver AR, Randall AD, Benham CD, & Pangalos MN (2002). mRNA distribution analysis of human TRPC family in CNS and peripheral tissues. *Brain Res Mol Brain Res* **109**, 95-104.

Rohacs T (2007). Regulation of TRP channels by PIP(2). *Pflugers Arch* **453**, 753-762.

Schaefer M, Plant TD, Obukhov AG, Hofmann T, Gudermann T, & Schultz G (2000). Receptor-mediated regulation of the nonselective cation channels TRPC4 and TRPC5. *J Biol Chem* **275**, 17517-17526.

Semtner M, Schaefer M, Pinkenburg O, & Plant TD (2007). Potentiation of TRPC5 by Protons. *J Biol Chem* **282**, 33868-33878.

Sharif-Naeini R, Dedman A, Folgering JH, Duprat F, Patel A, Nilius B, & Honore E (2008). TRP channels and mechanosensory transduction: insights into the arterial myogenic response. *Pflugers Arch* **456**, 529-540.

Spassova MA, Hewavitharana T, Xu W, Soboloff J, & Gill DL (2006). A common mechanism underlies stretch activation and receptor activation of TRPC6 channels. *Proc Natl Acad Sci U S A* **103**, 16586-16591.

Strotmann R, Harteneck C, Nunnenmacher K, Schultz G, & Plant TD (2000). OTRPC4, a nonselective cation channel that confers sensitivity to extracellular osmolarity. *Nat Cell Biol* **2**, 695-702.

Strubing C, Krapivinsky G, Krapivinsky L, & Clapham DE (2001). TRPC1 and TRPC5 form a novel cation channel in mammalian brain. *Neuron* **29**, 645-655.

Suchyna TM, Johnson JH, Hamer K, Leykam JF, Gage DA, Clemo HF, Baumgarten CM, & Sachs F (2000). Identification of a peptide toxin from Grammostola spatulata spider venom that blocks cation-selective stretch-activated channels. *J Gen Physiol* **115**, 583-598.

Suchyna TM, Tape SE, Koeppe RE, Andersen OS, Sachs F, & Gottlieb PA (2004). Bilayer-dependent inhibition of mechanosensitive channels by neuroactive peptide enantiomers. *Nature* **430**, 235-240.

Suh BC & Hille B (2005). Regulation of ion channels by phosphatidylinositol 4,5-bisphosphate. *Curr Opin Neurobiol* **15**, 370-378.

Suzuki M, Mizuno A, Kodaira K, & Imai M (2003). Impaired pressure sensation in mice lacking TRPV4. *J Biol Chem* **278**, 22664-22668.

Thastrup O, Cullen PJ, Drobak BK, Hanley MR, & Dawson AP (1990). Thapsigargin, a tumor promoter, discharges intracellular Ca2+ stores by specific inhibition of the endoplasmic reticulum Ca2(+)-ATPase. *Proc Natl Acad Sci U S A* **87**, 2466-2470.

Trebak M, Lemonnier L, Dehaven WI, Wedel BJ, Bird GS, & Putney JW, Jr. (2008). Complex functions of phosphatidylinositol 4,5-bisphosphate in regulation of TRPC5 cation channels. *Pflugers Arch.*

Venkatachalam K & Montell C (2007). TRP channels. *Annu Rev Biochem* **76**, 387-417.

Viana F, de la PE, Pecson B, Schmidt RF, & Belmonte C (2001). Swelling-activated calcium signalling in cultured mouse primary sensory neurons. *Eur J Neurosci* **13**, 722-734.

Voets T & Nilius B (2007). Modulation of TRPs by PIPs. *J Physiol* **582**, 939-944.

Voets T, Talavera K, Owsianik G, & Nilius B (2005). Sensing with TRP channels. *Nat Chem Biol* **1**, 85-92.

Vriens J, Watanabe H, Janssens A, Droogmans G, Voets T, & Nilius B (2004). Cell swelling, heat, and chemical agonists use distinct pathways for the activation of the cation channel TRPV4. *Proc Natl Acad Sci U S A* **101**, 396-401.

Watanabe H, Vriens J, Prenen J, Droogmans G, Voets T, & Nilius B (2003). Anandamide and arachidonic acid use epoxyeicosatrienoic acids to activate TRPV4 channels. *Nature* **424**, 434-438.

Wu D, Huang W, Richardson PM, Priestley JV, & Liu M (2008). TRPC4 in rat dorsal root ganglion neurons is increased after nerve injury and is necessary for neurite outgrowth. *J Biol Chem* **283**, 416-426.

Xu SZ, Sukumar P, Zeng F, Li J, Jairaman A, English A, Naylor J, Ciurtin C, Majeed Y, Milligan CJ, Bahnasi YM, Al-Shawaf E, Porter KE, Jiang LH, Emery P, Sivaprasadarao A, & Beech DJ (2008). TRPC channel activation by extracellular thioredoxin. *Nature* **451**, 69-72.

ACKNOWLEDGMENTS

We thank A. Miralles, E. Quintero, S. Ingham and G. Expósito for technical assistance, H. Cabedo, C. Morenilla-Palao and M. Pertusa for molecular biology advice, E de la Peña for

help with tissue extraction and A. Mälkiä and P. McNaughton for critical reading of the manuscript and helpful discussions. We also thank D. Clapham for mouse TRPC5, T. Plant for rat H_1 receptor and P. Majerus for the 5ptase IV cell line. The monoclonal antibody TRPC5 was obtained from the U C Davis /NINDS/NIMH NeuroMab Facility.A.G. is a "Ramón y Cajal" Investigator from the CSIC. This work was supported by funds from the Spanish Ministerio de Educación y Ciencia grants BFU2005-03986 (to AG), BFU2007-61855 (to FV) and CONSOLIDER-Ingenio 2010 Program (CDS2007-023).

FIGURE LEGENDS

Fig. 1. Hypoosmotic-induced membrane stretch activates TRPC5 channel. Pseudocolor images of GFP-TRPC5-transfected cells showing GFP-fluorescence (A) and ratiometric $[Ca^{2+}]_i$ responses to control (B) and 210 mOsm (C) solutions. Changes in $[Ca^{2+}]_i$ are reflected by the ratio of fura-2 emission at 340 versus 380 nm excitation wavelength (see color bar). Scale bar, 50 μm. (D) Time course of the calcium changes during hypoosmotic solution exposure in cells transfected with TRPC5 and in non-transfected cells (E) in the same field. The image 1C corresponds to the time course of calcium increase indicated by the arrow in figure 1D. For each experiment, 50-75 cells in the field were selected at random and identified as GFP(+) and GFP(–). (F) Percentage of cell responding to 210 mOsm solution exposure in cells expressing TRPC5 under the indicated experimental condition (***, $P < 0.001$,*Z*-test; each condition in >3 independent experiments). The (*) denotes statistical significance between cells transfected with TRPC5 in the absence of calcium, untransfected cells and cells transfected with the empty vector versus cell transfected with TRPC5 in the presence of extracellular calcium. (G) Bar histograms summarizing the responses of TRPC5 positive cells after incubation with 2μM thapsigargin compared with cell incubated with 2μM DMSO in a number of cells > 150 in six independent experiments (**P < 0.001; Z-test).

Fig. 2. Osmolarity-dependence of responsive cells in fura-2-loaded HEK293 cells expressing TRPC5. (A) $[Ca^{2+}]_i$ changes in response to reduction in extracellular osmolarity from 300 mOsm/Kg to the indicated values (for these set of experiments the fura-2 fluorescence was measured at its isosbestic point). (B-F) Bar histograms summarising the percentage of responsive cells and the mean evoked $[Ca^{2+}]_i$ elevation after consecutive steps in hypoosmolarity at the same cell (B, C; n= 576) and after application of one of the indicated

solution (E, F; n=271 for 260 mOsm, n=187 for 210 mOsm and n=45 for 170 mOsm). ** $P <$ 0.01; ***P < 0.001; Z-test and One way ANOVA). In B and E the asterisks denote statistical significance compared to maximal response obtained (170 mOSm/kg). In C and F the comparison were made between the experimental conditions.

Fig. 3. Osmotically-induced whole cell currents in cells expressing TRPC5. (A) Representative experiment showing the peak whole-cell current, measured at ± 80 mV, obtained from ± 100 mV voltage ramps in a cell expressing TRPC5 during application of 210 mOsm solution (B) I–V relationships obtained in control solution and at maximal current from the same cell as in (A). (C) Summary of the mean increase in current obtained in responsive cells to hypoosmotic stimulation (n= 67 cells) measured at -80 and +80 mV. (D) Whole-cell current (± 100 mV voltage ramps) in cell expressing TRPC5 during exposure to 210 mOsm solution in the presence and absence of extracellular calcium. (E) I–V relationship from the same cell as in (D) in the different experimental conditions. (F) Histogram summarizing the amplitude of the whole-cell current in TRPC5-expressing cells responding to hypoosmotical solution in the presence and absence of calcium, and different EGTA pipette concentrations from the type of experiment shown in (D). * $P < 0.01$ and *** $P < 0.001$ compared to responses in 2.4 mM external calcium (Student's t-test).

Fig. 4. The tarantula peptide GsMTx-4 inhibits the activation of TRPC5 by hypoosmotical stimulation. (A) Whole-cell currents evoked by hypoosmotic solutions in a TRPC5 transfected cell pre-incubated for 20 minutes with 5 μM GsMTx-4 before recording. (B) Responses to 100 μM histamine in a cell transfected with TRPC5 and H_1 receptor in the presence of GsMTx-4 and after wash out of the toxin.; same pre-incubations as in A. (C-D) I–V relationships corresponding with the time points marked in colors in A and B respectively. (E) Bar histogram summarizing the effect of GsMTx-4 on the percentage of responsive cells the block of the cell responses to hypoosmotic stimulation and histamine in control solution and in the presence of the toxin (* $P < 0.05$, compared with non-treated cells; Z-test). (F) The increases in current of the responsive cells measured at -80 and + 80 mV are summarised at the histogram. ** $P < 0.01$ compared with control cells for each type of stimulation (Student's *t*-test).

Fig. 5. Gating of TRPC5 by hypoosmotical stimulation is independent of phospholipase C activation. TRPC5-transfected cells were pre-incubated for 30-60 minutes with 5 μM of the PLC inhibitor U-73122 or the inactive analog U-73343. Thereafter cells were probed with 210 mOsm extracellular solution and 10 μM carbachol (Cch). (A) I–V relationship of TRPC5 current evoked by hypoosmotic solution and 10 μM carbachol (Cch) in the presence of 5 μM U-73122. (B) Effect of U-73122 and U-73343 on percentage of responsive cells to hypoosmotical stimulus and Cch compared to untreated TRPC5(+) cells obtained from the type of recordings shown in (A). **, $P < 0.01$, compared with non-treated cells and #, $P < 0.05$ compared with U-73343 treated cells (Z-test; n ≥ 6 patches for each condition). (C) Bar histogram summarizing the effects of U-73122 and U-73343 on TRPC5 currents induced by hypoosmotic solution and 10 μM Cch. Mean values were measured in > 6 cells for each experimental condition (*P < 0.05, the (*) denotes statistical significance between cells treated with U-73122 and untreated cells and (#) between cells treated with U-73343 and untreated cells; One way ANOVA). (D) Cytosolic Ca^{2+} signals from cells transfected with TRPC5 in response to 210 mOsm solution in the presence of ACA. (E) Whole-cell current obtained from ± 100 mV voltage ramps in a cell expressing the TRPC5 channel during the exposure of 210 mOsm solution in the presence of ACA. Note the current activation by ACA. (F) I–V relationship measured at maximal current from the same cell as E (colour dots) during the different experimental conditions (n = 4 patches).

Fig. 6. TRPC5 activation is strongly impaired in PIP_2-depleted cells. Time course of whole-cell currents in cells expressing TRPC5 channels during exposure to 210 mOsm solution and 500 μM ATP in a non-treated (A) and a tetracycline-treated cell (C). (B,D) I–V relationship measured at maximal current (colour dots) from the same cells as A and C respectively. (E) I–V relationship of the current evoked by hypoosmotic stimulation and 500 μM ATP in a tet-treated cell recorded with 10 μM $diC_8PI(4,5)P_2$ in the patch pipette (n=10). (F) Bar histogram summarising the results obtained in experiment shown in A-E. ***, $P < 0.001$ significance for tet-treated cells versus non-treated cells and #, $P < 0.05$ significance for tet-treated cells versus tet-treated cell recorded with 10 μM $diC_8PI(4,5)P_2$ in the patch pipette (Z-test). (G) Mean evoked current increment at -80 and +80 mV activated by hypoosmotical solution and ATP in the same conditions than Fig. F. *, $^{\#}$ P < 0.05 significance for non-treated cells versus tet-treated cells and non-treated cells versus tet-treated cell recorded with 10 μM $diC_8PI(4,5)P_2$ in the patch pipette respectively (One way ANOVA). *** $P< 0.001$

significance for tet-treated cells versus non-treated cells (Student's *t*-test). (H-I) Representative $[Ca^{2+}]_i$ signals obtained in non-treated and tet-treated cells transfected with TRPC5 in response to 210 mOsm solution and 500 μM ATP. (J) Bar histogram summarizing the effect of PIP_2 depletion from type experiments shown in H-I. *** denotes the $P < 0.001$ significance (Z-test) for the hypoosmotic and ATP responses for non-treated (3 independent experiments) versus tet-treated cells (5 independent experiments). The number of the analyzed cells is indicated above each column.

Fig. 7. Pressure-induced stretch activation of TRPC5 channels.
(A) Representative time course of whole-cell current development induced by steps of positive pressure applied to the interior of HEK293 cell transfected with TRPC5. (B) I–V relationship obtained at maximal current from the same cell as in (A) (colour dots). (C) Mean evoked current increase to positive pressure (n = 19 patches). (D) Time course of whole-cell current in TRPC5-transfected cell induced by hypoosmotic solution and positive pressure. (E) I–V relationship obtained at maximal current from the same cell as in (D) (colour dots). Note the very similar shape of the I-V relationship in response to both stimuli. The applied pressure is indicated at the lower panel in A and D ranging from 10 to 50 mmHg. (E) Representative time course of whole-cell current development induced by steps of positive pressure applied to the interior of HEK293 cell transfected with the empty vector pCI-NEO.

Fig. 8. Expression of TRPC5 channels in primary sensory neurones. (A) RNA from trigeminal and dorsal root ganglia, hippocampus and HEK-293 cells was reverse transcribed (+) and PCR amplified with specific primers for murine and human TRPC5. The (-) symbols in the panels indicate the reactions for each RNA sample run in the absence of SuperScript II (see Methods). Water lines correspond to the PCR mix with water as a negative control for PCR amplification.
(B-E) Immunocytochemical staining of TRPC5 in dissociated mouse TG neurones visible in transmitted (B) and confocal microscopy (C) and for the secondary antibody visible in transmitted (D) and confocal microscopy (E). Anti-TRPC5 immunoreactivity is indicated in red and Hoechst nuclear staining in blue. TRPC5-positive neurones are indicated by arrows and -negative by arrowheads. Scale bar 10 μm. (F) Histogram of TG cell size distribution of TRPC5-immunoreactive cells.

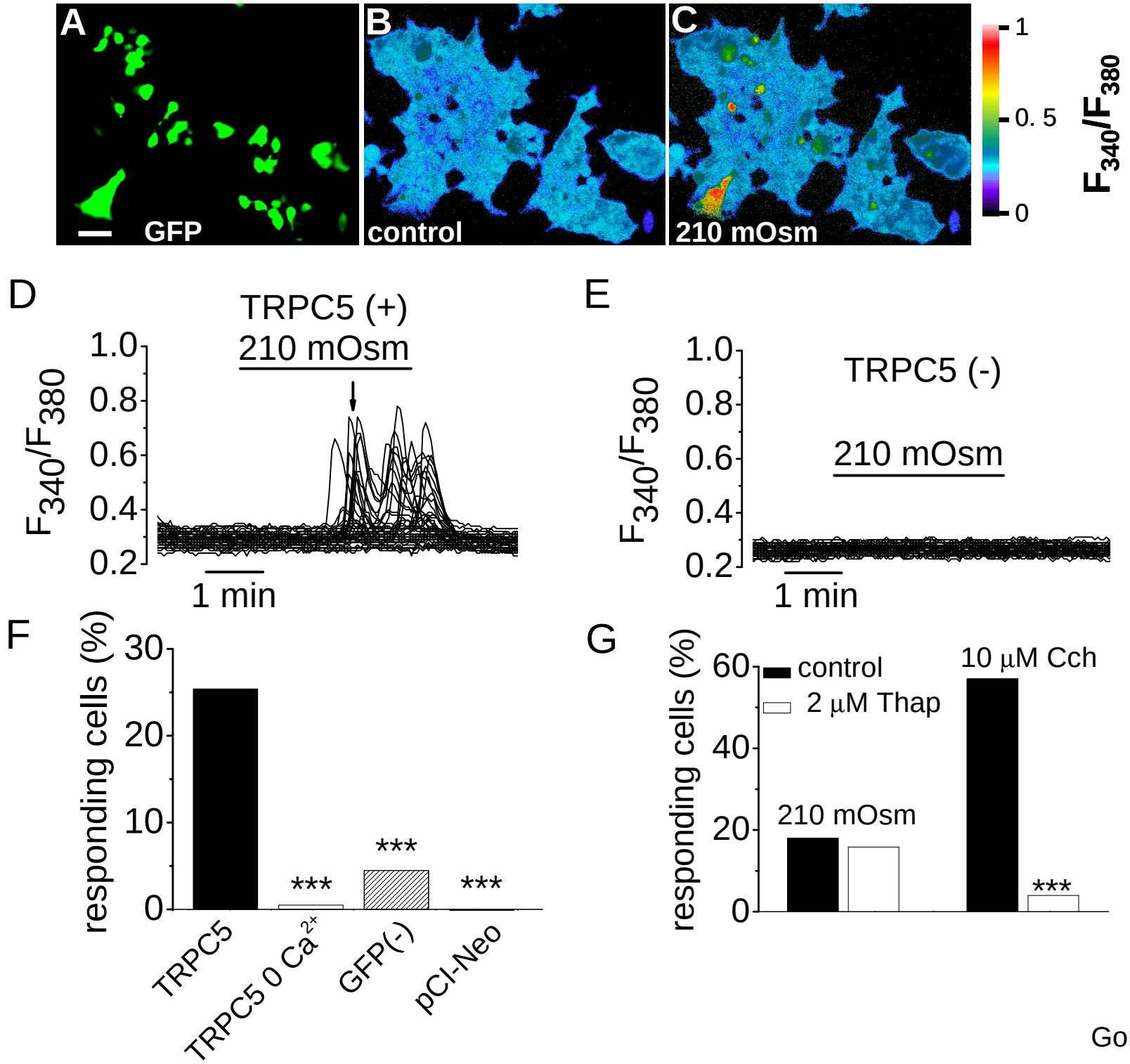

Gomis et al. Fig. 1

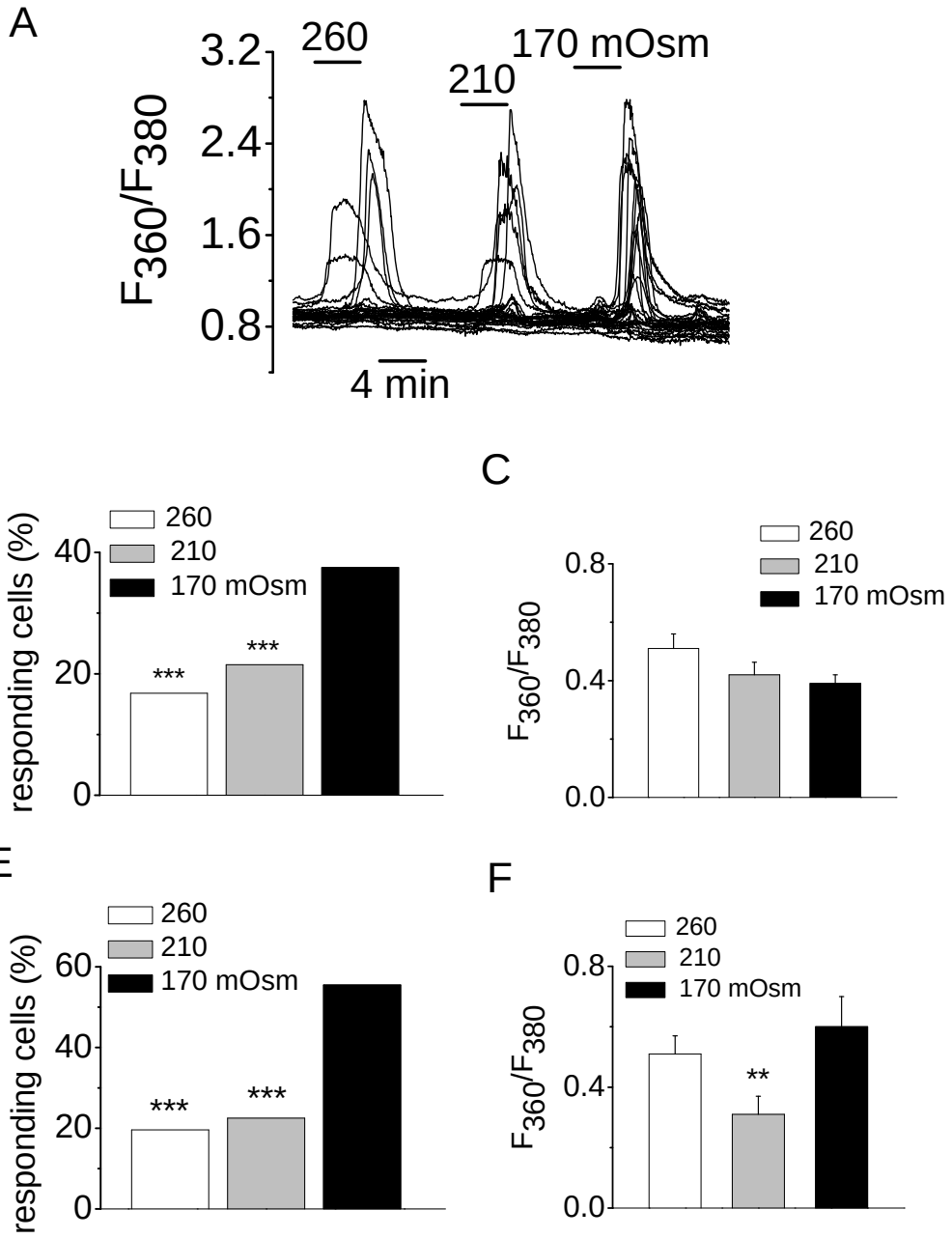

Gomis et al. Fig. 2

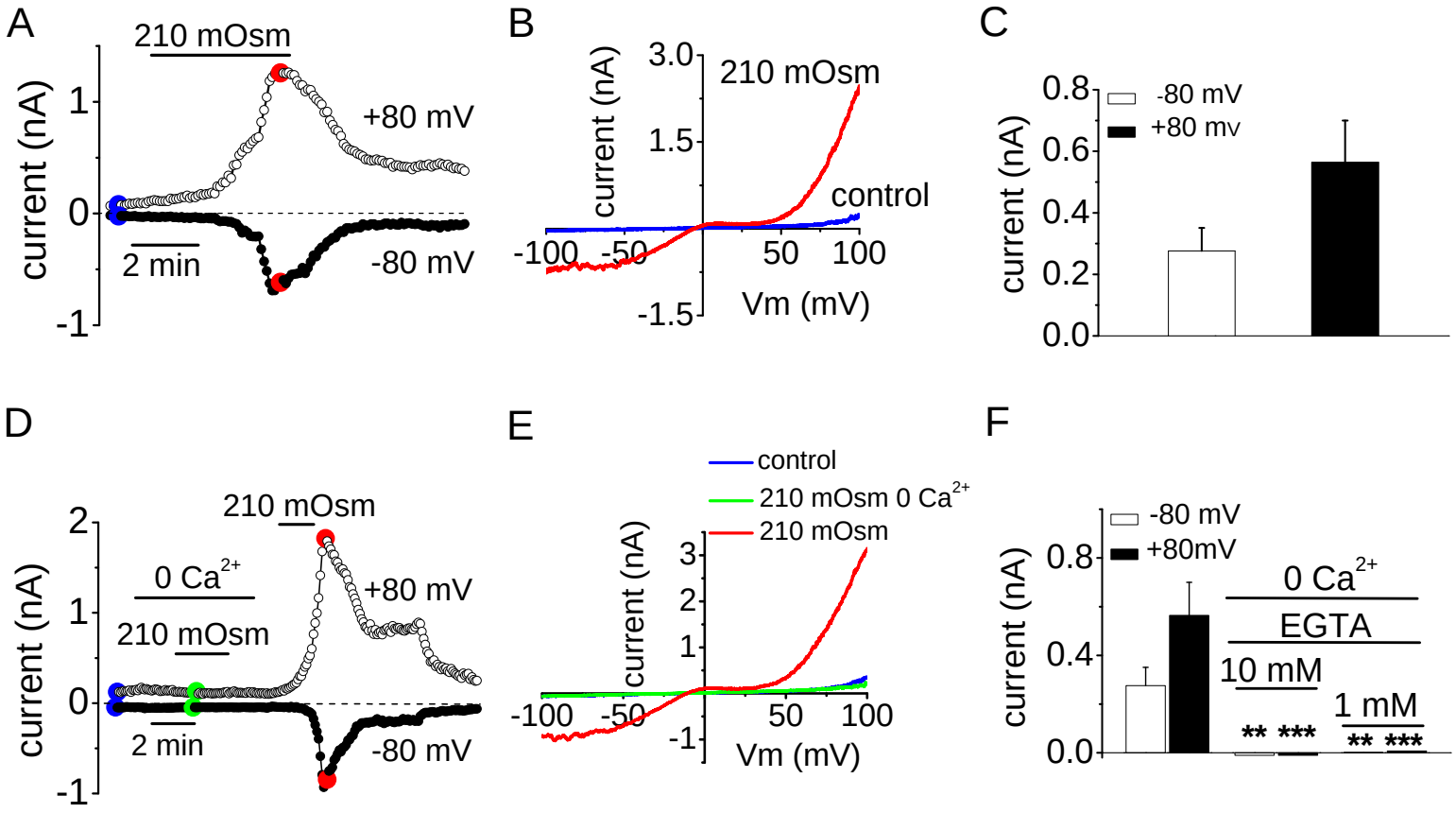

Gomis et al. Fig. 3

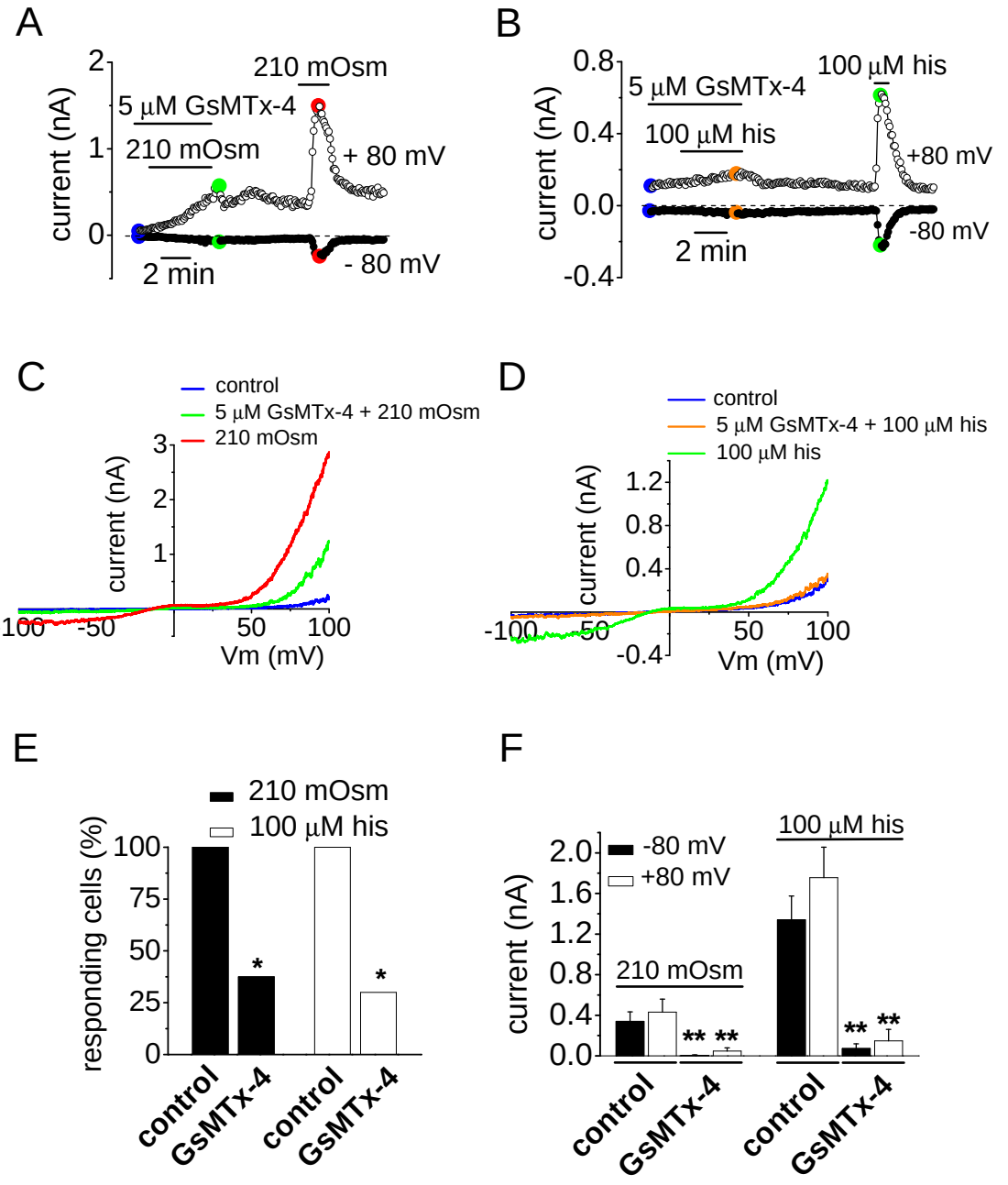

Gomis et al. Fig. 4

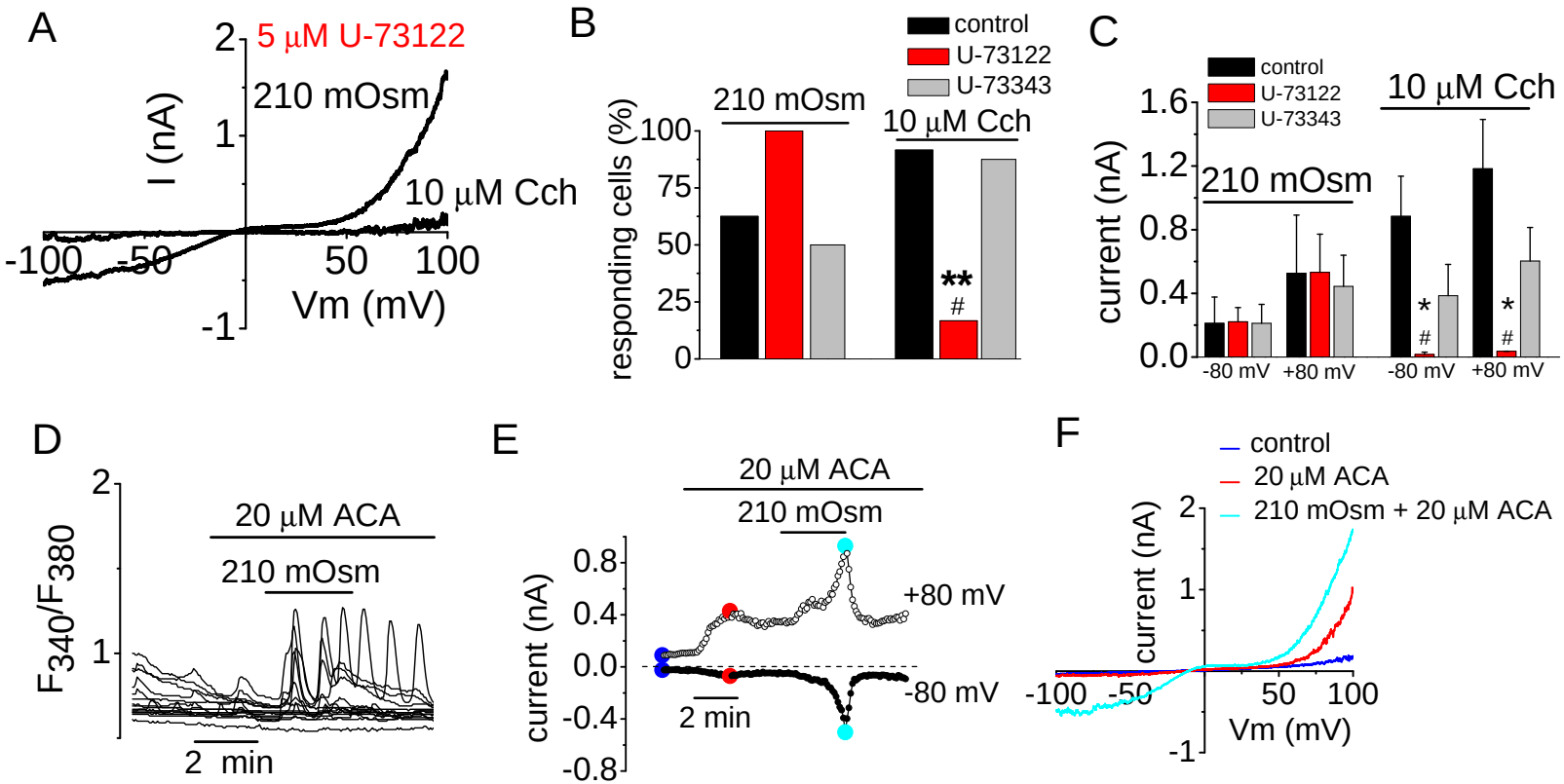

Gomis et al. Fig. 5

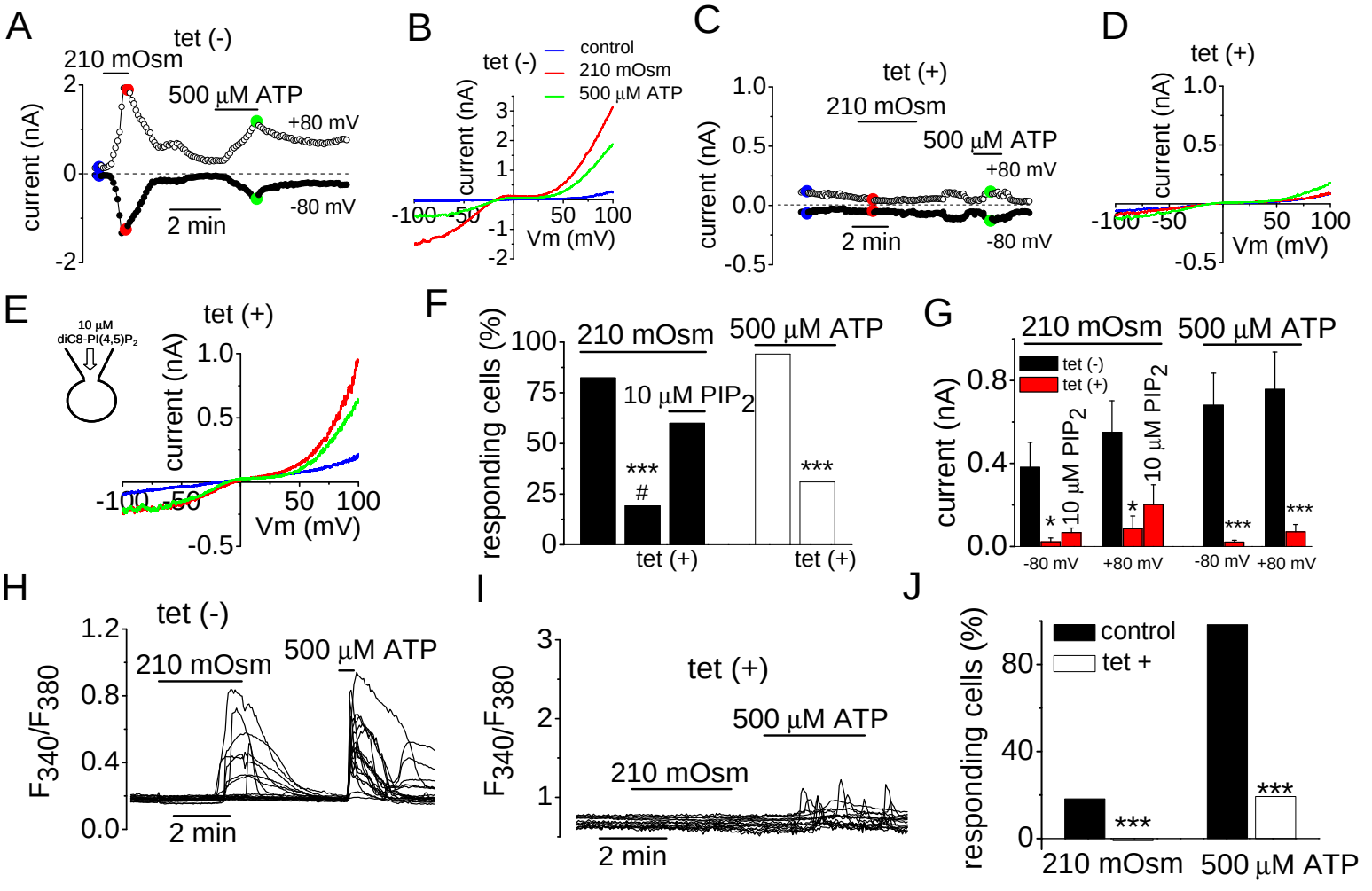

Gomis et al. Fig. 6

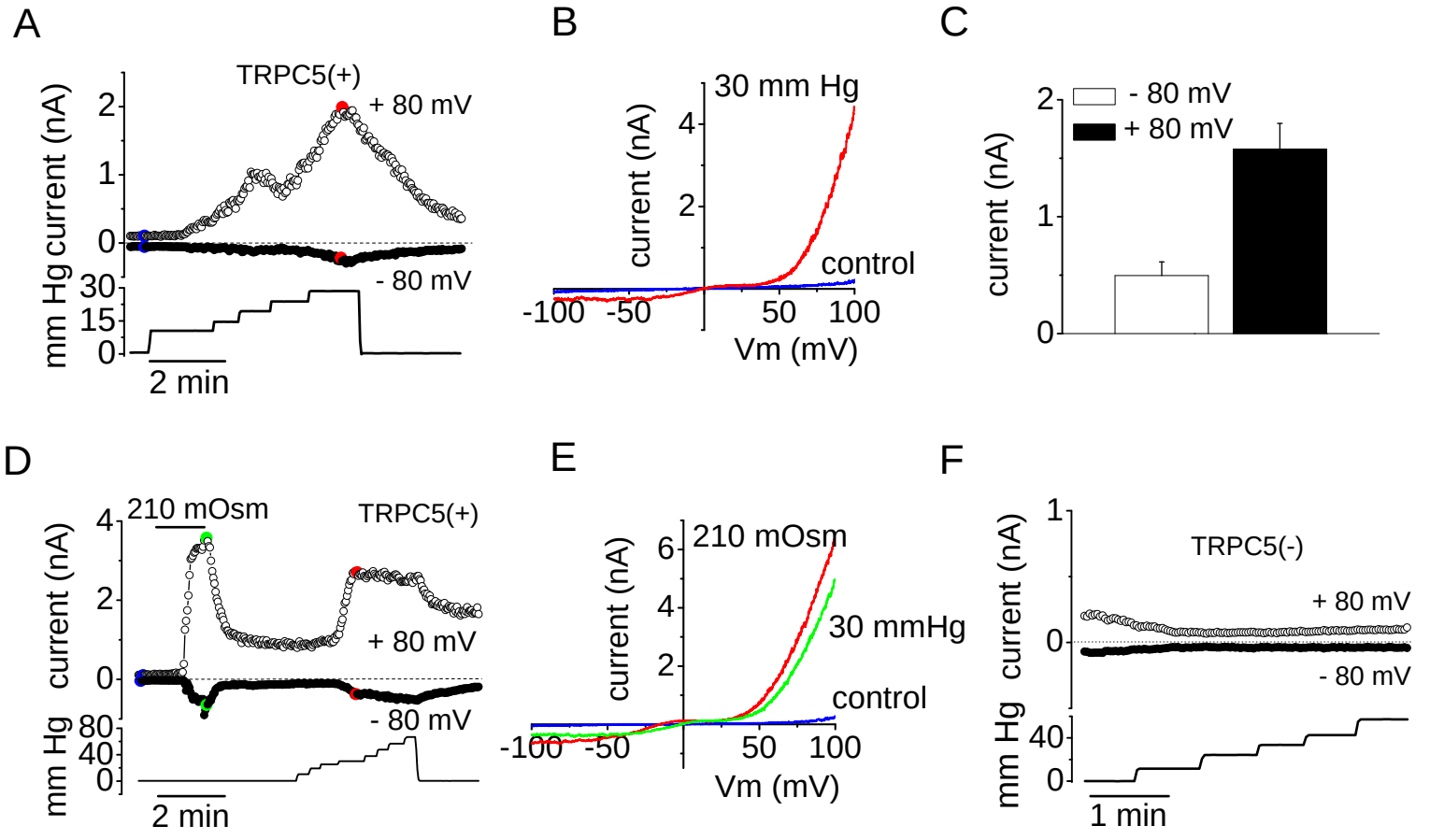

Gomis et al. Fig. 7

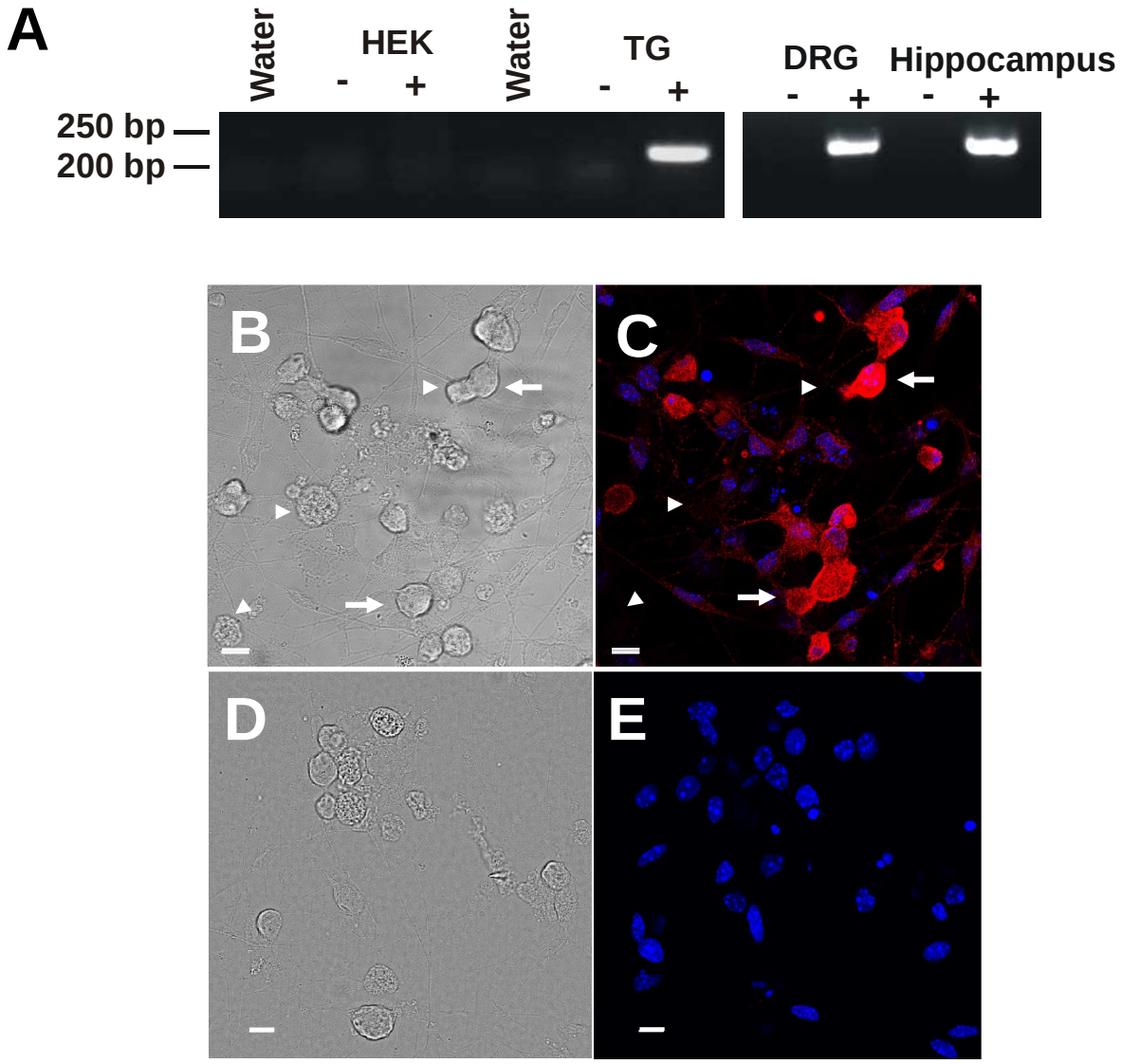

Gomis et al. Fig 8